ELSEVIER

Thermochimica Acta 320 (1998) 223–230

thermochimica acta

Thermal stability and dehydration of anapaite

S.G. Eeckhout[a], R. Vochten[b], N.M. Blaton[c], E. De Grave[a], J. Janssens[b], H. Desseyn[b,*]

[a] *NUMAT, Department of Subatomic and Radiation Physics, University of Gent, Gent, Belgium*
[b] *Chemistry Department, RUCA-University of Antwerp, Antwerpen, Belgium*
[c] *Laboratory for Analytical Chemistry and Medicinal Physicochemistry, Catholic University of Leuven, Leuven, Belgium*

Received 7 April 1998; received in revised form 15 June 1998; accepted 29 June 1998

Abstract

The thermal behavior of anapaite, $Ca_2Fe^{2+}(PO_4)_2{\cdot}4H_2O$, has been studied by TG/DTG and DSC techniques, complemented by Fourier-transform IR spectroscopy. The anapaite sample, originating from Bellaver de Cerdena (Spain) was identified as such using X-ray diffraction and qualitative energy-dispersive analysis of X-rays. ^{57}Fe Mössbauer spectroscopy at various temperatures could not detect any Fe^{3+}. It was found from thermal analyses and IR spectroscopy that two types of hydrogen–bonded water molecules exist in the structure. This feature is related to the distance between the hydrogen atom of a water molecule and the oxygen atom of a phosphate group, the distance between both oxygen atoms and the angle $O(H_2O)$–$H\cdots O(PO_4)$. The dehydration process proceeds in two partially overlapping steps. The removal of the last two, strongly bonded water molecules is accompanied by the decomposition of the crystal structure. From TG curves, the activation energy was calculated for different intervals of dehydration reaction. For this purpose, five slow heating rates between 0.4 and 2°C/min were applied. The activation energy for the entire process was also obtained from DSC (223 kJ/mol) and found to be in reasonable agreement with the average of the various values from the TGA (233 kJ/mol). The heat of reaction for the complete dehydration was found to be 177 kJ/mol. © 1998 Elsevier Science B.V.

Keywords: Activation energy; Anapaite; Dehydration; IR spectroscopy; Thermal stability

1. Introduction

Anapaite, $(Ca_2Fe^{2+}(PO_4)_2{\cdot}4H_2O)$, shows a green or yellowish green color and a glasssy lustre. The platy crystals belong to the triclinic system and crystallise in P $\bar{1}$ [1]. The unit-cell parameters are a=6.447(1), b=6.816(1), c=5.898(1) Å, α=101.64(3), β=104.24(3), γ=70.76(4)° and Z=1. The mineral possesses a three-dimensional framework structure. The Ca, Fe and P atoms exhibit an eight-, a six- and a four-fold co-ordination, respectively. The iron is bound to four basal water molecules and to two apical oxygen atoms belonging to a phosphate tetrahedron. Each Ca atom is surrounded by six oxygen atoms, which belong to four different phosphate tetrahedra, and by two water molecules. Two unit cells of the anapaite structure are displayed in Fig. 1.

The unit-cell contains four H_2O molecules, each of which coordinates to a ferrous cation. In general, the strength of the hydrogen bonding depends on three parameters, namely (1) the distance between the hydrogen atom of a water molecule and the oxygen atom of a phosphate group, (2) the distance between both oxygen atoms and (3) the angle between

*Corresponding author.

PII S0040-6031(98)00446-8

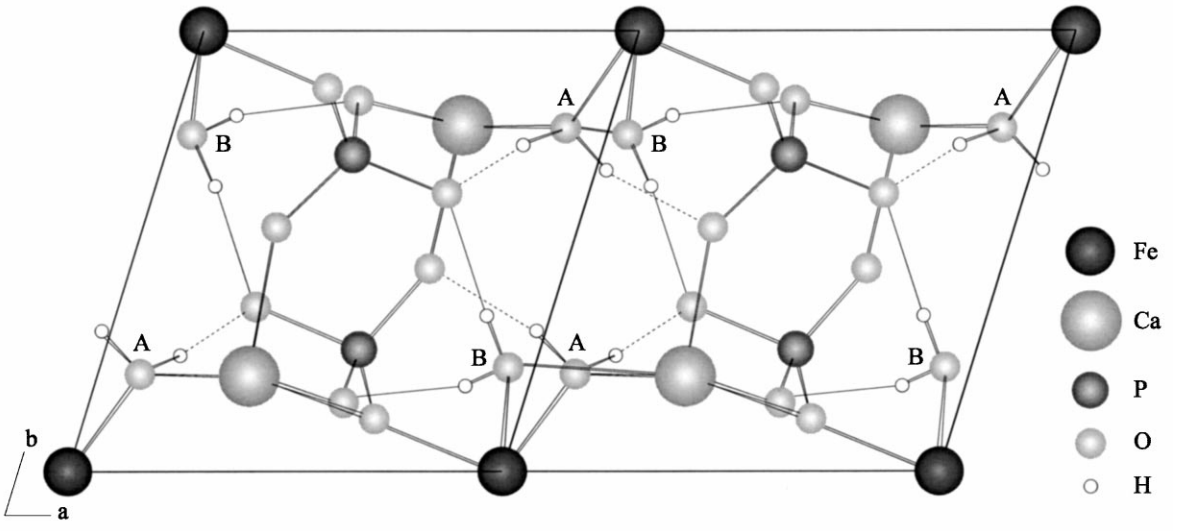

Fig. 1. Schematic representation of the crystal structure of anapaite. Two unit cells are displayed and the strong (- - -) and weak (———) hydrogen bonds are marked.

Table 1
Classification into strong (A) and weak (B) water molecules in the anapaite structure according to the $H(H_2O)$–$O(H_2O)$ distance in Å, the $O(H_2O)$–$O(PO_4)$ distance in Å and the O–H···O angle in °

	H–O/Å	O–O/Å	O–H···O/°	H–O/Å	O–O/Å	O–H···O/°
A	1.72	2.60	174	1.77	2.60	160
B	1.86	2.72	170	1.96	2.79	162

$O(H_2O)$–H···$O(PO_4)$. According to these parameters, two types of hydrogen bonds are distinguished: strong and weak ones. A water molecule with only strong or only weak hydrogen bonds will hereafter be called an A and a B water molecule, respectively. The bond characteristics are listed in Table 1 for both types of water molecules. The strong hydrogen bonds are continuously linked to form parallel chains lying in the (100) plane, whereas the weak hydrogen bonds link two such parallel chains along the *c*-axis (see Fig. 1). A and B water molecules are in trans-position in the basal plane of the iron coordination octahedron. The vertices of this octahedron are occupied by oxygens belonging to a phosphate tetrahedron. Ca has an eight-fold coordination polyhedron.

In spite of the large number of general data published on the hydrogen bonding in O–H···O systems [2], the chemical factors determining its absolute strength remain uncertain, but, for the O–H···O system a relationship between the O···O distance and the hydrogen–bonding strength in a practical linear O–H···O system is generally accepted. Novak [3] classified this type of hydrogen bonding as weak for O···O distances greater than 2.70 Å, intermediate for distances between 2.70 and 2.60 Å and strong for O···O distances shorter than 2.60 Å. For linear or nearly linear systems (i.e. O–H···O angle $\geq 165^\circ$), Gille et al. [4] recently defined very strong hydrogen bonds as those being shorter than 2.50 Å, strong ones between 2.50–2.65 Å, medium ones between 2.65–2.80 Å and weak ones for distances greater than 2.80 Å. From this classification the two different hydrogen bonds in anapaite can be regarded as medium to strong. This hydrogen bonding and the coordination of the water molecules to the iron cation predict a thermally stable compound which only dehydrates at higher temperatures. Finally, Catti et al. [1] reported on an anapaite whose TG curve

apparently exhibits only one step of dehydration at ca. 200°C, but a double maximum for the corresponding DTG curve.

2. Experimental

For this study, anapaite of Bellaver de Cerdena, Spain was used. The green crystals, present in small geodes of dolomitized limestone, were carefully hand-picked under the microscope. X-ray diffraction data of sieved anapaite crystal fragments (<150 μm) as well as anapaite ground at room temperature and in ice water were recorded at 40 kV and 20 mA, with FeK_α radiation (λ=1.9373 Å) using a Phillips diffractometer PW1730/10. Silicon powder (NBS-640) was used as internal standard. Qualitative energy-dispersive analysis of X-rays was performed on a JSM-6400 Scanning Electron Microscope combined with a JXA-6400 microprobe. Mössbauer spectra (MS) were collected at various temperatures in transmission mode with a constant-acceleration drive and a triangular reference signal. The MS were fitted with symmetric, Lorentzian-shaped doublets. IR spectra in KBr were recorded on a Bruker Vector 22 FTIR instrument. Thermal analyses were performed on TA Instruments: TG/DTG on a TA 2950 and DSC on a TA 2920. All measurements were run on ~6 mg of small single crystals under a N_2 stream of 50 ml/min between room temperature and 600°C at different heating rates. To calculate the activation energy (E_a) from TGA, the method of Ozawa [5] was used. According to this method, E_a is calculated for discrete fractional extents (α) of the dehydration reaction from curves recorded at different heating rates (β). To get reliable results, five heating rates were used to calculate the straight line ln $\beta = f(1/T_\alpha)$ the slope of which yields E_a. In order to get optimum separation of the two steps in the dehydration process, low heating rates were used, namely 0.4, 0.6, 0.8, 1.0 and 2.0°C/min. The method of Ozawa [5] was also applied to calculate E_a from DSC curves recorded at the same heating rates as the TG curves. To construct the plot ln $\beta = f(1/T_{min})$, the temperatures corresponding to peaks (T_{min}) in the DSC curves were used. The reaction heat (ΔH) for the dehydration process was directly calculated from the DSC curve since the software of the controller system, after calibrating the instrument based on the fusion heats of pure metals, links areas under a curve with heat flow and thus with heat of reaction.

3. Results and discussion

3.1. XRD, EDAX and Mössbauer spectroscopy

The X-ray diffraction pattern (XRD) of small crystal fragments (<150 μm) shows the reflections of anapaite (JCPDS 34-148). Qualitative energy-dispersive analysis of X-rays (EDAX) of several selected crystal fragments revealed the presence of Ca, Fe and P. No trace elements could be detected. ^{57}Fe Mössbauer spectroscopy at various temperatures (4.2–420 K) could not detect any Fe^{3+}.

The unit-cell parameters of anapaite calculated by Catti et al. [1] are a=6.447(1), b=6.816(1), c=5.898(1) Å, α=101.64(3), β=104.24(3), γ=70.76(4)° and Z=1. The crystal structure of the studied crystals was refined in space group P $\bar{1}$ with the program PIRUM [6]. The obtained unit-cell parameters are a=6.448(1), b=6.816(1), c=5.898(1) Å, α=101.65(1), β=104.26(2), γ=70.75(3)° and Z=1. The least-squares refinement program was further used for the X-ray diffraction patterns of anapaite ground at room temperature and in ice water. The unit-cell parameters are a=6.453(1), b=6.813(2), c=5.900(1) Å, α=101.65(2), β=104.28(1), γ=70.75(2)°, Z=1 and a=6.448(1), b=6.816(1), c=5.899(1) Å, α=101.65(1), β=104.27(1), γ=70.76(2)°, Z=1, respectively. In conclusion, the values obtained for the crystals and for both powders are the same within the error range (3σ) as those calculated by Catti et al. [1].

3.2. IR spectroscopy

The interpretation of vibrational spectra of water has been the subject of numerous discussions [7–9]. The extremely complicated spectra are the result of intermolecular hydrogen–bonding and coupling effects.

The IR spectrum of anapaite and of the water-free compound are displayed in Fig. 2. In the vibrational spectrum of anapaite, two different kinds of water molecules are clearly distinguished, each of which exhibits a stretching vibration ν_{OH}, a bending vibra-

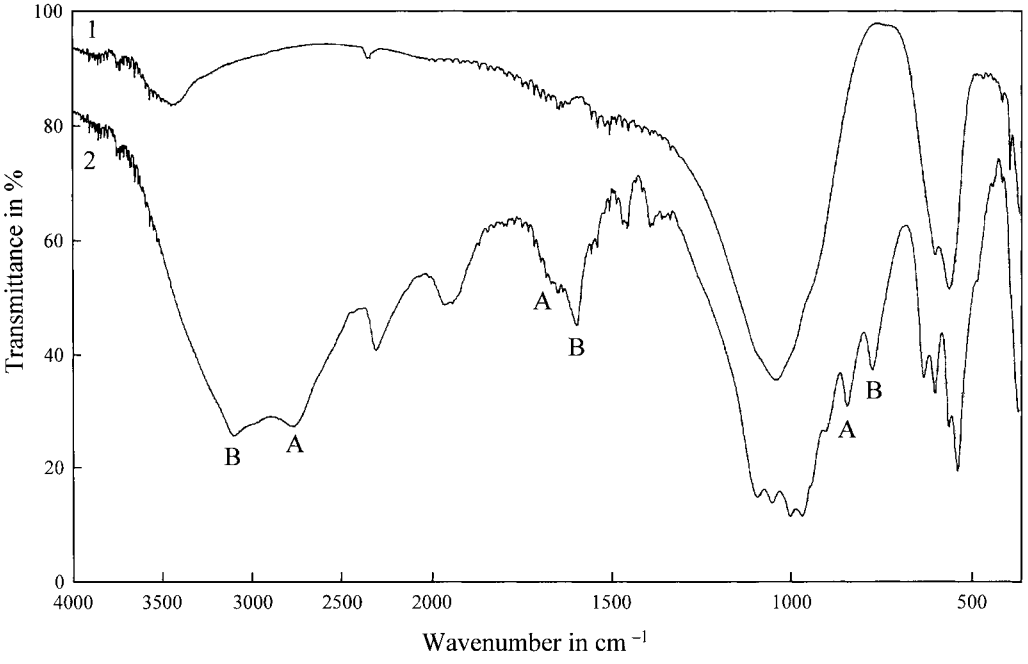

Fig. 2. Fourier transform IR spectra of anapaite (2) and of water-free anapaite (1). A refers to the type A water molecules and B to the type B water molecules.

tion δ_{OH} and an out-of-plane tilting τ_{OH}. The two types of water molecules do not form hydrogen bonds with each other. According to the ν_{OH} frequencies, Novak [3] classified weak hydrogen bonds as those exhibiting ν_{OH} modes in the 3400–3200 cm^{-1} region, intermediate ones in the 3200–2800 cm^{-1} region and strong ones with ν_{OH} modes below 2700 cm^{-1}. The two absorption bands observed at 3096 and 2769 cm^{-1} are assigned to the ν_{OH} modes of the B type and A type of water molecules, respectively, indicating the stronger hydrogen bonding for the A type. This feature is also reflected in the δ_{OH} modes, namely at 1597 cm^{-1} for the B type and at 1652 cm^{-1} for the A type and in the τ_{OH} modes, namely at 776 cm^{-1} for the B type and at 846 cm^{-1} for the A type. The latter ones are exceptionally clearly observed and disappear in the water-free compound. The distinct splitted bands in the 1000 and 500 cm^{-1} region in the anapaite spectrum are assigned to the ν_{PO} and δ_{PO} modes, respectively. These splitting effects are absent in the spectrum of the water-free compound, confirming the decomposition of the crystal structure by total dehydration.

3.3. Thermal analyses

The relatively large difference in hydrogen–bonding strength between the H_2O molecules of types A and B suggests a different thermal stability and, consequently, a differentiation in the dehydration. This difference however can only be observed at low heating rates, as shown in Fig. 3 where the TG curves of anapaite recorded at a heating rate of 0.4 and 20°C/min are displayed. The TG curve at very low heating rate (0.4°C/min) reveals a total loss of weight of 17.6% corresponding to four water molecules. This process occurs in two slightly overlapping steps without forming a real plateau. The same feature is observed in the DTG curve (see Fig. 3) with maxima at 231° and 267°C and in the DSC curve (see Fig. 4) with minima at 235° and 269°C. The activation energies (E_a) calculated by the method of Ozawa [5] from TG curves recorded at different heating rates, and this for nineteen intervals (α) of the dehydration reaction, are shown in Table 2 and in Fig. 5. The corresponding correlation coefficients to the straight line defined by $\ln \beta = f(1/T_\alpha)$ are also given. From this table, it can be

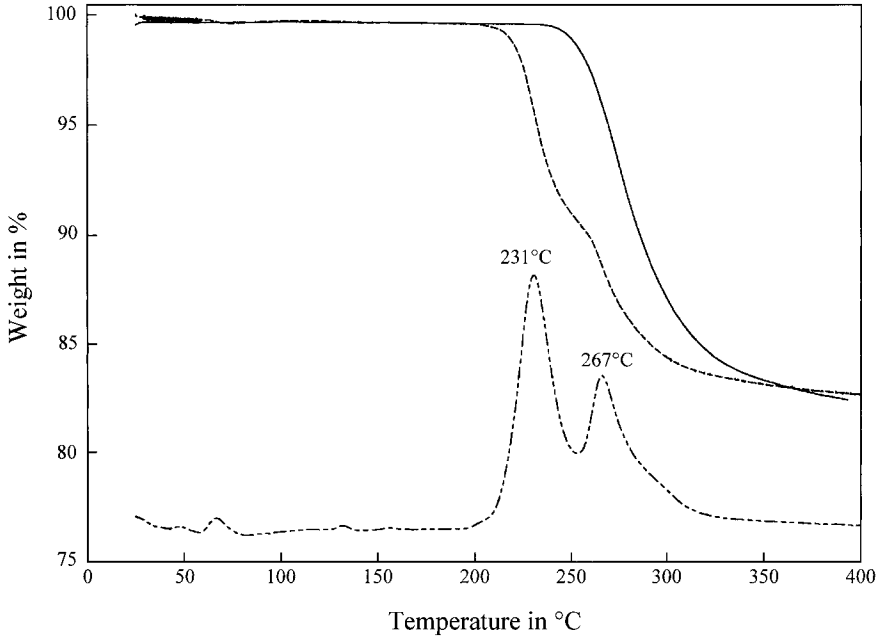

Fig. 3. TG curves of anapaite crystal fragments recorded at a heating rate of 20°C/min (———), of 0.4°C/min (- - -) and DTG (– – –) curve of anapaite recorded at a heating rate of 0.4°C/min.

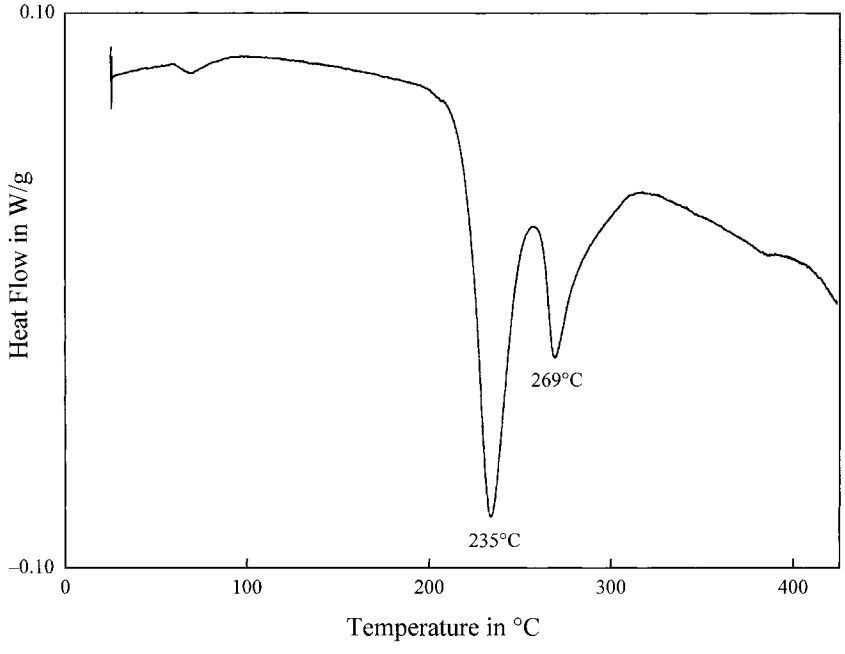

Fig. 4. DSC curve of anapaite recorded at a heating rate of 0.4°C/min.

Table 2
Activation energies (E_a) in kJ/mol calculated by the method of Ozawa [5] for nineteen fractional extents (α) of the dehydration reaction from TG curves recorded at different heating rates (β) and their corresponding correlation coefficients to the straight line ln β=f(1/T_α)

α	E_a/(kJ/mol)	Correl. coeff
0.05	185.5	0.990
0.10	188.9	0.988
0.15	191.1	0.989
0.20	194.4	0.989
0.25	196.0	0.990
0.30	198.9	0.990
0.35	203.2	0.990
0.40	209.4	0.990
0.45	222.4	0.986
0.50	252.2	0.973
0.55	296.3	0.965
0.60	294.1	0.995
0.65	262.9	0.996
0.70	250.5	0.996
0.75	250.2	0.993
0.80	258.3	0.989
0.85	274.9	0.981
0.90	265.7	0.953
0.95	218.0	0.772
Mean	233±38	

deduced that during the first part of the reaction (α=0.0–0.4), when the main loss of the type B water molecules takes place, E_a increases slowly and almost linearly from 185 to 210 kJ/mol. Once the bonds are broken, the water molecules have to diffuse through the crystal, hence the small increase in E_a. A second part in the reaction can be defined at α values between 0.4 and 0.6, where the final fraction of the type B water molecules is released and the removal of the type A water molecules simultaneously starts. At this stage E_a rises from ~210 to ~300 kJ/mol, probably due to the chemical and physical forces that are needed to decompose the crystal structure and to release the more strongly bounded water molecules. For α values above 0.6, the calculated E_a is scattering between 250 and 300 kJ/mol because of the dominating effect of the decomposition of the crystal structure. This feature was also concluded from the IR spectra. The last value for E_a (at α=0.95) has not been considered since the corresponding correlation coefficient is too small (0.772).

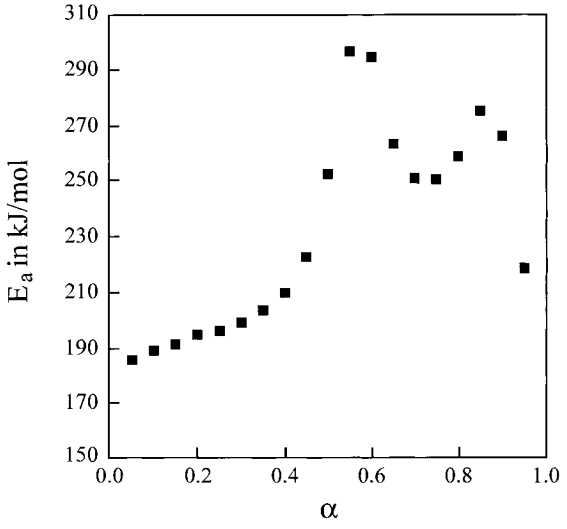

Fig. 5. Activation energies in kJ/mol for the dehydration of anapaite calculated by the method of Ozawa.

The activation energy was also calculated by the method of Ozawa [5] from DSC curves recorded at different heating rates. The obtained value for the entire dehydration process is 223 kJ/mol and the corresponding correlation coefficient to the straight line defined by ln β=f(1/T_{min}) is 0.996. This value for E_a is in reasonable agreement with the average of the values calculated from TGA, namely 233±38 kJ/mol. The activation energy for the first part of the reaction (α=0.0–0.4) calculated from DSC is 196±8 kJ/mol. This value is comparable to the ones obtained from TGA which is found to be between 185 and 210 kJ/mol.

The reaction heat (ΔH) for the complete dehydration was directly determined from the DSC curve. These values are presented in Table 3 for DSC runs at different heating rates. The mean value for ΔH is 177±9 kJ/mol.

The values for E_a obtained for the removal of the type B water molecules and the values for ΔH are in agreement with those for dehydration of hydrogen–bounded molecules coordinated to a metal ion [10–12].

3.4. Effect of grinding

Anapaite crystal fragments, as well as anapaite ground at room temperature and ground in ice water

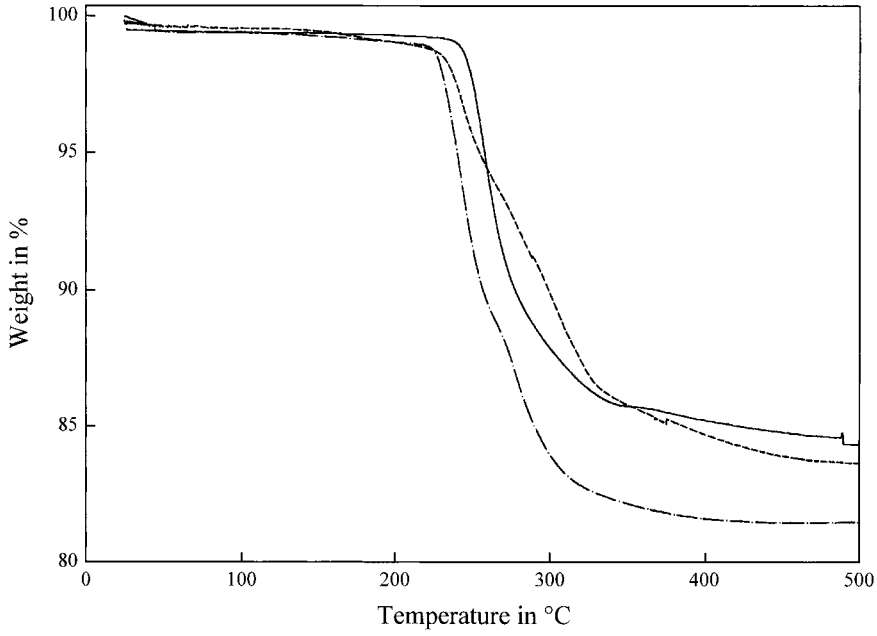

Fig. 6. TG curves at a heating rate of 1.0°C/min of anapaite crystal fragments (– · –), anapaite ground at room temperature (———) and ground in ice water (- - -).

Table 3
The heat of reaction (ΔH/(kJ/mol)) for the complete dehydration of anapaite determined from DSC at different heating rates (β) between 0.4° and 2.0°C

β/(°C/min)	ΔH/(kJ/mol)
0.4	182.6
0.6	183.0
0.8	174.7
1.0	162.7
2.0	183.1
Mean	177±9

were heated up to 600°C at 1.0°C/min. The TG curve of the crystals shows two partially overlapping dehydration steps with a total loss of weight of 17.6%, corresponding with 4 mol of H_2O. The powder ground at room temperature contains 3 mol of H_2O, whereas the powder ground in ice water has 3.5 mol of H_2O. All three TG curves are shown in Fig. 6. In conclusion, anapaite looses H_2O on grinding.

However, since the XRD patterns of small anapaite crystal fragments and of both ground samples are the same, it is concluded that the removal of the type B water molecules takes place without decomposition of the crystal structure. This is confirmed by the values of E_a for the release of the first two water molecules (α=0.0–0.4). IR results from the water-free anapaite however show that the removal of the four water molecules requires the destruction of the crystal structure. This feature is also reflected in the E_a values which are scattered between 250 and 300 kJ/mol for α=0.4–0.9.

From X-ray powder patterns obtained with a high-temperature Guinier camera between 20° and 700°C, Catti et al. [1] concluded that the anapaite phase disappears at ca. 267°C. The ν_{OH}, δ_{OH} and τ_{OH} modes are, consequently, absent from the IR spectrum of the water-free compound. This spectrum also proves that the crystal splitting of the phosphate mode is no longer observed due to the decomposition of the crystal structure.

Acknowledgements

The authors wish to thank the Fund for Scientific Research – Flanders for financial suppport. Mrs. G. Thijs is thanked for preparing the manuscript.

References

[1] M. Catti, G. Ferraris, G. Ivaldi, Bull. Minéral. 102 (1979) 314.
[2] P.O. Kollman, L.C. Allen, Chem. Rev. 72 (1972) 283.
[3] A. Novak, Structure and Bonding 18 (1974) 177.
[4] P. Gille, V. Bertolozi, V. Ferretti, G. Lille, J. Am. Chem. Soc. 116 (1994) 909.
[5] T. Ozawa, J. Thermal Anal., 2 (1970) 301; 7 (1975) 601.
[6] P.E. Werner, Arkiv Kemi 31 (1969) 513.
[7] M. Falk, J. Raman Spectrosc. 21 (1990) 563.
[8] M. Falk, Spectrochim. Acta 40 (1984) 43.
[9] H.O. Desseyn, M. Hereygers, S.P. Perlepes, J. Raman Spectrosc. 26 (1995) 77.
[10] M. Hereygers, H.O. Desseyn, S.P. Perlepes, K.A. Verhulst, A.T.H. Lenstra, J. Chem. Crystallography 24(9) (1994) 615.
[11] C. Vansant, H.O. Desseyn, V. Tangoulis, C.P. Raptopoulou, A. Terzis, S.P. Perlepes, Polyhedron 14, 15–16 (1995) 2115.
[12] J. Ribas, A. Escuer, M. Serra, R. Vicente, Thermochimica Acta 102 (1986) 125.